

Distinguishing between Triplet-Pair State and Excimer Emission in Singlet Fission Chromophores Using Mixed Thin Films

Julian Hausch, Adam J. Berges, Clemens Zeiser, Tim Rammmer, Arne Morlok, Jona Bredehoff, Sebastian Hammer, Jens Pflaum, Christopher J. Bardeen,* and Katharina Broch*



Cite This: *J. Phys. Chem. C* 2022, 126, 6686–6693



Read Online

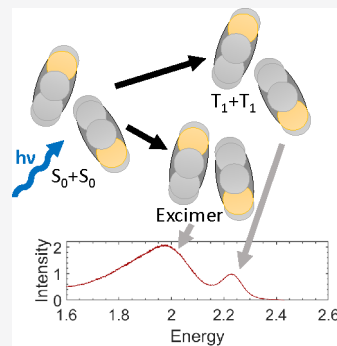
ACCESS |

Metrics & More

Article Recommendations

Supporting Information

ABSTRACT: In the photoluminescence spectra of thin films made of singlet fission (SF) materials emission features that are red-shifted from the free exciton emission are of particular interest. They can be fingerprints of the correlated triplet-pair state and as such offer insights into the mechanisms of the multistep SF process. However, excimer formation or trap-state population can also cause such features and a clear disentanglement of the various contributions can be challenging. Here, we use blends of anthradithiophene (ADT) and weakly interacting organic semiconductors to control the polarizability of the molecular environment and, thus, to distinguish between excimer emission and emission from the correlated triplet-pair state. Using time-resolved photoluminescence spectroscopy measurements, we clarify the relation between excimer formation and SF in ADT and find that excimer formation constitutes a parallel relaxation channel for the exciton and neither mediates nor hinders SF.



INTRODUCTION

In the optimization of organic optoelectronic devices, a crucial part is understanding the mechanism and contribution of loss channels. To obtain deeper insight into the involved processes, photoluminescence (PL) spectroscopy is a well suited method, as it not only allows the detection of nonradiative channels via quenching but also is sensitive to specific radiative channels such as the population of trap states or excimer formation, both of which can be readily identified by spectroscopic signatures red-shifted from the exciton emission.^{1,2} Similar signatures are of particular importance for a specific class of organic semiconductors, namely singlet fission (SF) materials, as they can give insights into the details of this multistep, technologically relevant,³ process. SF describes the spin-allowed fission of a singlet exciton into two triplet excitons via an electronically coupled triplet-pair state (¹(TT)) of singlet character⁴ and has been successfully studied *inter alia*^{5–7} via PL spectroscopy to elucidate the nature of the triplet-pair state intermediate and the related pathways of triplet-pair formation and triplet separation.^{8–16}

However, one complication that arises in the investigation of SF materials by PL spectroscopy is the fact that the intermediate ¹(TT) state is a dark state¹⁷ that becomes only emissive via Herzberg–Teller coupling.^{13,15,18–20} The resulting red shift of the corresponding emission compared to the energy of the ¹(TT) state leads to an overlap of its spectral signature with other contributions at low photon energies such as excimers^{2,11,12,14,21–26} or trap-state emission.^{1,13–15} This poses the experimental challenge to disentangle the various contributions leading to emission features at low photon energies (in the following referred to as red-shifted

luminescence features (RSL)) and to clarify whether the related states mediate SF^{10,12,16,21,27–29} or constitute a loss channel.^{11,14,15,22,23,25,30–34} This question directly relates to an ongoing debate in the literature, which concerns the role of excimer formation in the SF process.^{11,12,14,21–26,31,34} Excimers as a competing channel for SF have been observed experimentally in tetracene (TET)^{11,14,34,35} and anthradithiophene (ADT) derivatives,^{20,30} but have also been proposed as an intermediate state for SF.^{10,27,36,37}

The challenges preventing a general elucidation of the nature of the many possible states which can cause RSL (X_{RSL}) in thin films of SF materials arise from the above-mentioned ambiguity in the assignment of spectral signatures^{10,13,16,20,34} and the lack of a tunable parameter that affects the energetic position of trap state emission, ¹(TT) state emission, and excimer emission differently. Here, we address this open question in ADT, a chromophore whose derivatives have been reported to exhibit both SF and pronounced RSL.²⁰ ADT is codeposited with two spacer compounds to continuously change the intermolecular interactions, the number of nearest neighbors, and the polarizability of the local molecular environment. The spacer molecules TET and 6-phenacene (6PH) are chosen to have singlet energies greater than that of

Received: October 26, 2021

Revised: March 21, 2022

Published: April 8, 2022



ADT, making energy transfer from ADT to the spacers unlikely. The resulting changes in the dynamics of the different decay channels are probed by time-resolved PL spectroscopy (TRPL). Comparing the photoluminescence behavior of ADT in blends with spacer molecules of high and low polarizability,³⁸ TET and 6PH (see Figure 1a), respectively, with

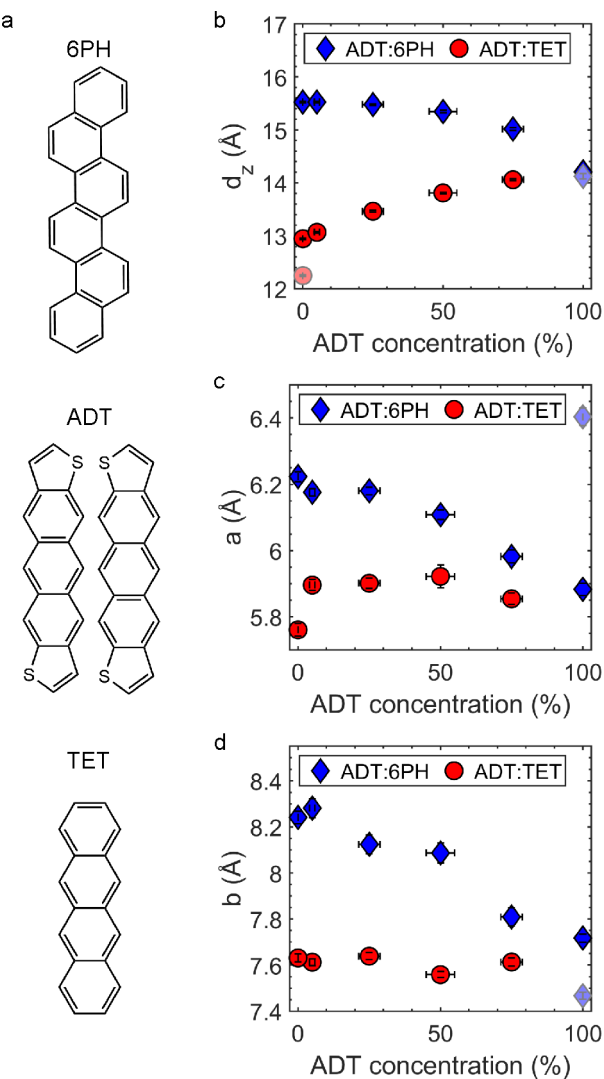


Figure 1. (a) Chemical structure of the investigated molecules. For ADT, the two isomers present in our samples are shown, see Supporting Information for details. (b) Out-of-plane lattice spacing and (c,d) in-plane unit cell parameters (c) a and (d) b , determined by X-ray diffraction. The faded data points indicate the unit cell parameters determined for the second polymorph of ADT or TET (see Supporting Information for details). Note that the in-plane unit cell parameters do not differ significantly between the two polymorphs of TET.

ADT in solution, allows us, first, to confirm the occurrence of SF in ADT and, second, to distinguish between spectral contributions of the ${}^1(\text{TT})$ state, trap states and excimers. We identify the latter as a parallel pathway to SF in ADT, allowing for a refinement of current models on the role of X_{RSL} debated in the literature.^{13,14}

METHODS

Anthradithiophene (ADT, Sigma-Aldrich, 97% purity, the material contains a mixture of two different isomers, anti-ADT and syn-ADT (chemical structures are displayed in Figure 1a); see Supporting Information for details), Tetracene (TET, Sigma-Aldrich, 99.99% purity), and [6]-phenacene (6PH, Lambson Japan Co. Ltd., 99% purity) were used as received. The samples were prepared by codeposition (organic molecular beam deposition) in a high vacuum chamber with a base pressure of 10^{-8} mbar. The molecules were resistively heated in individual Knudsen-cells, and the deposition rate for each molecule was controlled by a separate quartz crystal microbalance (QCM), calibrated using X-ray reflectivity (XRR) measurements. All films have a nominal thickness of 80 nm and were deposited with a total growth rate of 6 Å/min on native silicon and quartz glass substrates, which were kept at room temperature during growth. The mixing ratio of each film was calculated in molar % of ADT. XRR measurements were performed on a Ge XRD 3003TT instrument, and grazing incidence wide-angle X-ray scattering (GIWAXS) measurements, on a Xeuss 2.0 (Xenocs) in-house instrument with a Pilatus 300k detector, both using Cu K_α radiation ($\lambda = 1.541$ Å). Absorption spectra were recorded with a PerkinElmer Lambda 950 UV-vis-NIR spectrometer. The steady-state PL measurements were conducted with a pulsed laser diode LDH-P-C-470 (Pico-Quant, Germany) of 470 nm wavelength, a time-averaged power of $0.05 \mu\text{W}$, and a repetition rate of 40 MHz. Using a Plan-NEOFLUAR 65x/NA 0.75 air-objective (Carl Zeiss AG, Germany), the laser pulses were focused on a spot with a $30 \mu\text{m}$ diameter on the sample, yielding a fluence of $1.77 \times 10^{-4} \mu\text{J}/\text{cm}^2$. As the detecting unit, an Acton SP300 spectrometer with a PIXIS 100 camera (both Princeton Instruments, USA) was used.

Time-resolved photoluminescence measurements were taken with a Hamamatsu C4334 Streakscope having a time resolution of 20 ps and a spectral resolution of 2.5 nm. The 800 nm output of an 80 MHz Coherent Vitesse Ti:sapphire oscillator was frequency doubled to generate the 400 nm excitation pulse. A Pockels cell controlled by a ConOptics pulse-picking system was used to adjust the repetition rate of the oscillator to 100 kHz. A 450 nm long wave-pass filter was placed before the streak camera to minimize the contribution of laser light scatter to the signal. All measurements were performed in a vacuum cryostat (10^{-5} Torr) fitted with optical windows, and pulse fluences remained below $1.2 \mu\text{J}/\text{cm}^2$.

RESULTS AND DISCUSSION

The commercially available ADT used in our work contains two isomers (anti-ADT and syn-ADT; see Figure 1a for chemical structures). However, this does not significantly impact our results as both isomers show similar structural and optical properties as derived from X-ray diffraction experiments³⁹ and DFT calculations (see Table S1 in the Supporting Information). Consequently, we do not expect differences in the steric compatibility, the mixing behavior, or the intermolecular interactions of the two ADT isomers with the spacer molecules (TET and 6PH) studied here. Also, most previous studies on optical and electronic properties of ADT and its derivatives use a mixture of both isomers as well.^{13,40-44} In the following we will thus refer to the isomerically mixed material as ADT. The structural properties of the two mixed systems (ADT:TET blends and ADT:6PH blends) are

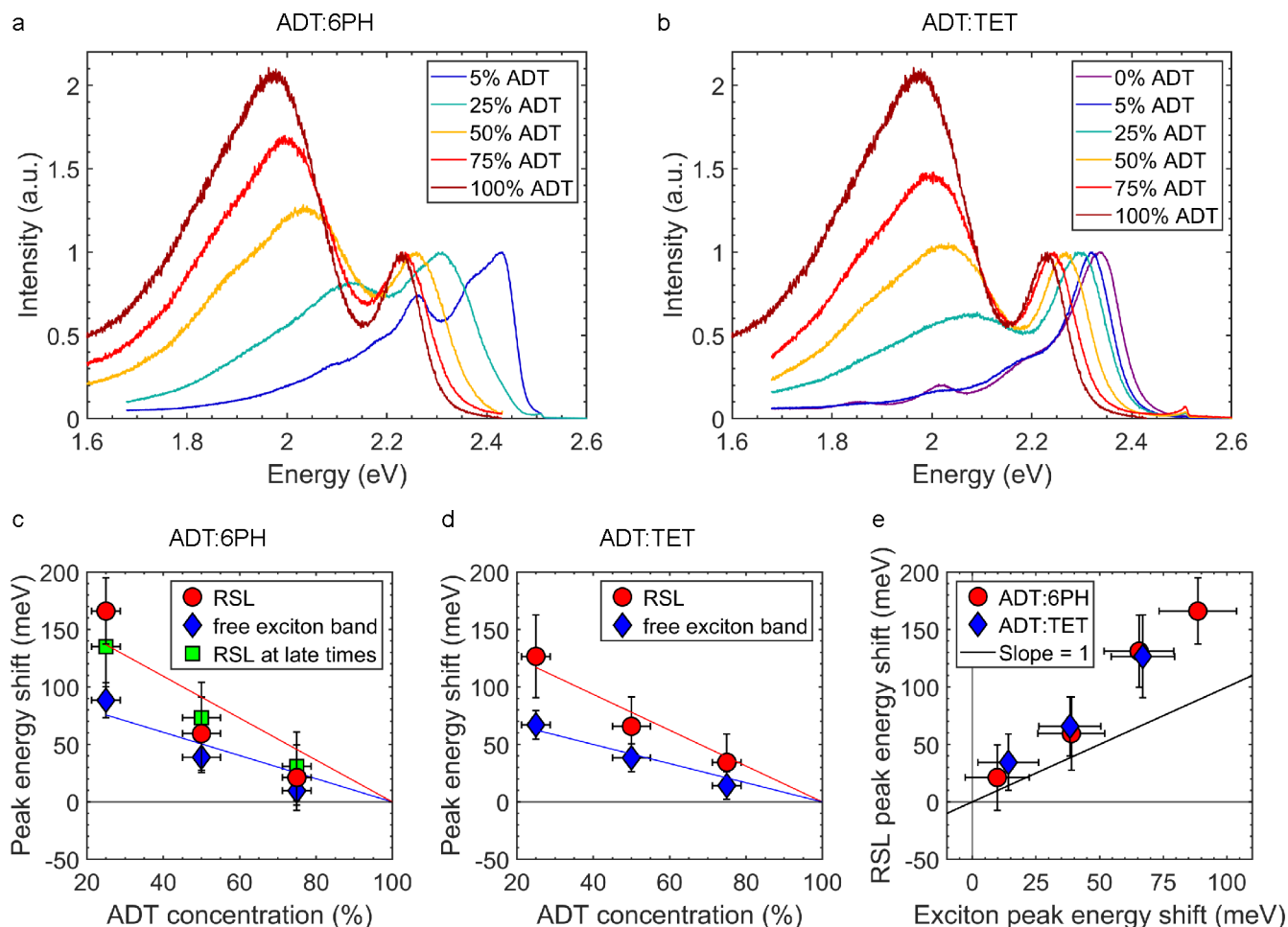


Figure 2. (a,b) Quasi-steady-state PL spectra of ADT:6PH (a) and ADT:TET blends (b) with different mixing ratios. The photon energy of the excitation was 2.54 eV. (c,d) Energetic shift of the RSL, the RSL at late times and the exciton peak position in ADT:6PH (c) and ADT:TET (d) blends compared to the respective positions for neat ADT. The red and blue lines are guide to the eye for the peak shift of the exciton (blue) and the RSL (red), respectively. (e) Energetic shift of the RSL against the shift of the free exciton emission for ADT:6PH and ADT:TET.

summarized in Figure 1b–d. For both a continuous change in the out-of-plane lattice spacing is observed, suggesting statistical intermixing⁴⁵ (see Figures S1–S3 in the Supporting Information for details), but there are clear differences in the dependence of the in-plane unit cell parameters a and b on the ADT concentration. While these parameters continuously increase with decreasing ADT concentration in blends with 6PH, they remain constant in blends of ADT with TET. This is consistent with statistical intermixing and with the fact that the neat ADT and TET films have comparable in-plane unit cell sizes, while it is clearly larger for neat 6PH (Figure 1c,d). Since the in-plane unit cell parameters describe the plane in which the molecular interactions are strongest,⁴⁶ any changes in these parameters might affect the related intermolecular electronic coupling^{47–49} and, consequently, the photophysics. However, by comparing two mixed systems with different trends, we can estimate the impact of such structural changes on the PL spectra and the underlying excited state dynamics.

The steady-state PL spectra of the different samples are shown in Figure 2. The PL spectrum of neat ADT is dominated by two transitions, one at 2.21 eV, which we assign to emission of the free exciton based on the spectral shape and the small Stokes shift of 70 meV ($S_1 \leftarrow S_0$ in absorption at 2.28 eV; see Figure S4 in the Supporting Information). The second emission peak occurs at 1.95 eV, red-shifted by $\Delta E = 260$ meV

compared to the first emission peak. This spacing is too large for a vibronic progression of the free exciton, which we would expect around $\Delta E = 150$ meV based on the vibronic progression of the absorption spectrum (see Figure S4 in the Supporting Information), and we thus assign it to the before-mentioned RSL that has been observed also for other SF compounds.^{10,11,13,14,16,20,30}

Now considering the PL spectra of the blends, a first interesting result is the independence of the spectral shape on the codeposited compound and the dominant ADT contribution as can be seen in Figure 2a,b. The blends with 5% ADT are the exception, with a PL spectrum that resembles the solution spectrum of ADT (Supporting Information, Figure S7b) for blends with the high band gap spacer molecule 6PH, and is dominated by TET emission in the case of ADT:TET blends (see Supporting Information for details). In the following, we will restrict the discussion to blends with ADT concentrations above 5%. Comparing the positions of the two main features in neat ADT with their positions in the PL spectra of the blends (see Figure 2c–d), we observe a continuous shift to higher photon energies with decreasing ADT concentration in all cases, which can be explained by changes in the polarizability of the local molecular environment in the blends compared to the neat film. The absolute value of the shift follows the optical band gap of the spacer

molecules and the related polarizability,³⁸ since the observed shift is larger in blends of ADT with the high band gap (low polarizability) spacer molecule 6PH compared to the low band gap (higher polarizability) spacer molecule TET. Further comparing the shift of the free exciton emission and the RSL for all blends, we find that the shift is more pronounced for the latter (see trendlines in Figure 2c,d), implying that X_{RSL} is more sensitive to changes in the polarizability of the environment than the free exciton. This increased sensitivity can be rationalized by a stronger charge transfer (CT) state admixture,^{48–50} which has been observed for excimers^{31,51} and gives us first insight into the nature of X_{RSL} . An additional noteworthy finding is the decrease of the intensity of the RSL relative to the free exciton emission with decreasing ADT concentration. For processes which strongly depend on interactions between neighboring molecules, like excimer formation or triplet-pair state formation, such an intensity decrease results from the replacement of nearest ADT neighbors by TET as well as 6PH.⁵² Importantly, as the probability for a given number of ADT neighbors follows a binomial distribution⁵² and is thus independent of the molecule (TET or 6PH) replacing ADT, this intensity decrease is identical in ADT blends with TET or 6PH. To summarize these first results, the coexistence of the RSL with emission of the free exciton makes these ADT based blends an ideal model system to investigate the origin of the RSL and its impact on SF using TRPL measurements.

Time traces extracted at the energetic position of the free exciton emission and the RSL are shown in Figure 3 and have been analyzed by fitting to a biexponential decay (see Figure 4a,b and Table S2 in the Supporting Information for decay rates and Supporting Information for details). In thin films the free exciton emission decays generally faster than the RSL and, in addition, exhibits a higher sensitivity to changes in the ADT concentration. The rates of the free exciton decay decrease linearly with decreasing ADT concentration independent of the spacer molecule (see Figure 4a,b). This, in combination with an increased decay rate of the free exciton emission of a neat ADT thin film compared to ADT in solution (see Figure 3a) gives insight into the photophysics of ADT. In solution, ADT exhibits a decay rate of 0.57 ns^{-1} , while in the polycrystalline solid state a new, much more rapid decay process with a rate of about 42 ns^{-1} appears. Furthermore, the linear dependence of this decay rate on the ADT concentration in blends demonstrates that two nearest neighbors are involved in this rapid decay and that the increase in lateral spacing with decreasing ADT concentration plays a minor role. On these time scales, SF is the most probable candidate for this system, also because SF has already been reported to occur in a variety of ADT derivatives.^{13,20,30} Importantly, we can not only conclude that SF is the main decay path of the free exciton, but our results for ADT blends also allow us to elucidate its microscopic mechanism. The linear dependence of the SF rate on the chromophore concentration has been observed before for TET and referred to as the replacement effect,^{52,53} indicating that SF occurs via incoherent population transfer from S_1 to ${}^1\text{TT}$. The deviation from this linear dependence found for TET blends with low ADT fractions can be explained by the similar band gaps of ADT and TET, which makes an excitation of solely ADT impossible and can also enable an energy transfer from ADT to TET. Hence the excited state dynamics of TET have to be considered for these blends as well, which is done in the Supporting Information.

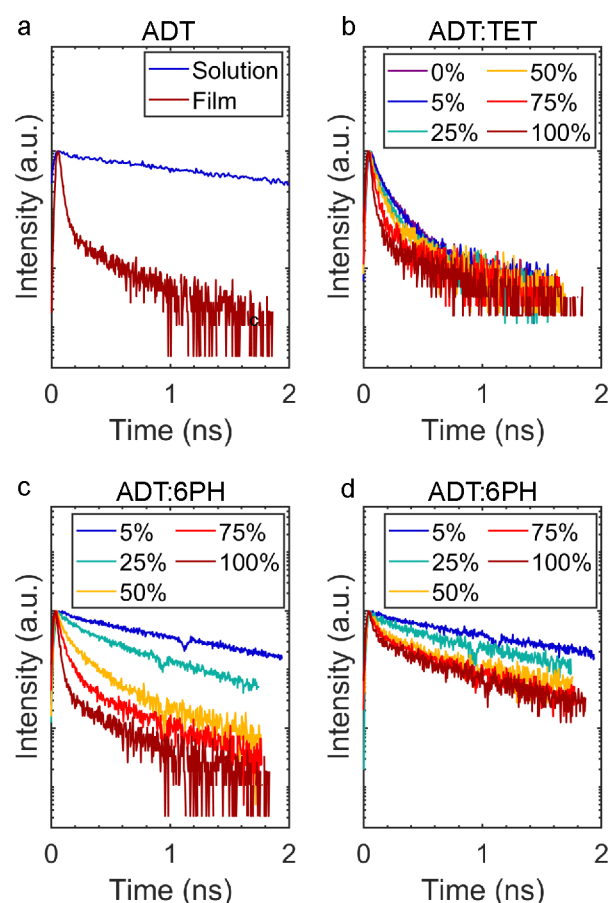


Figure 3. (a) Time traces of the singlet exciton emission of ADT in CHCl_3 solution and in a neat ADT film. (b,c) Time traces of the free exciton emission in (b) ADT:TET and (c) ADT:6PH blends with different ADT concentrations, (d) time traces of the RSL in ADT:6PH blends with different ADT concentrations. ADT concentrations of the blends are given in molar % in the legend. The intensity is scaled logarithmically.

Since SF is mediated by states comparable to X_{RSL} in ADT derivatives,^{13,20} the dynamics of the RSL also give insight into the SF mechanism. The temporal evolution of the RSL intensity (see Figure 3d and Figure S5 in the Supporting Information) allows us to conclude that X_{RSL} is formed on a time scale faster than the instrument response ($<10 \text{ ps}$) and, furthermore, that population transfer from the exciton to X_{RSL} can be excluded as the major decay channel for the free exciton due to the lack of an increase in RSL intensity on the time scale of the free exciton emission decay. Lastly, the intensity decay of the RSL follows a similar trend with changing ADT concentration as that observed for the free exciton (see Table S2 in the Supporting Information for numeric values), although less pronounced.

In order to shed further light on the decay dynamics, PL spectra of the different ADT:6PH blends have been extracted by integrating the intensity over two time windows. For the first, short time window, a time interval between 0 and 2 ns was chosen in which both the exciton emission and the RSL are observed for blends with ADT concentrations above 5%. The starting time for the second, longer time window was chosen individually for each blend such that the decay of the exciton emission was almost complete. A noteworthy result of the comparison of the spectra in these two time windows is the

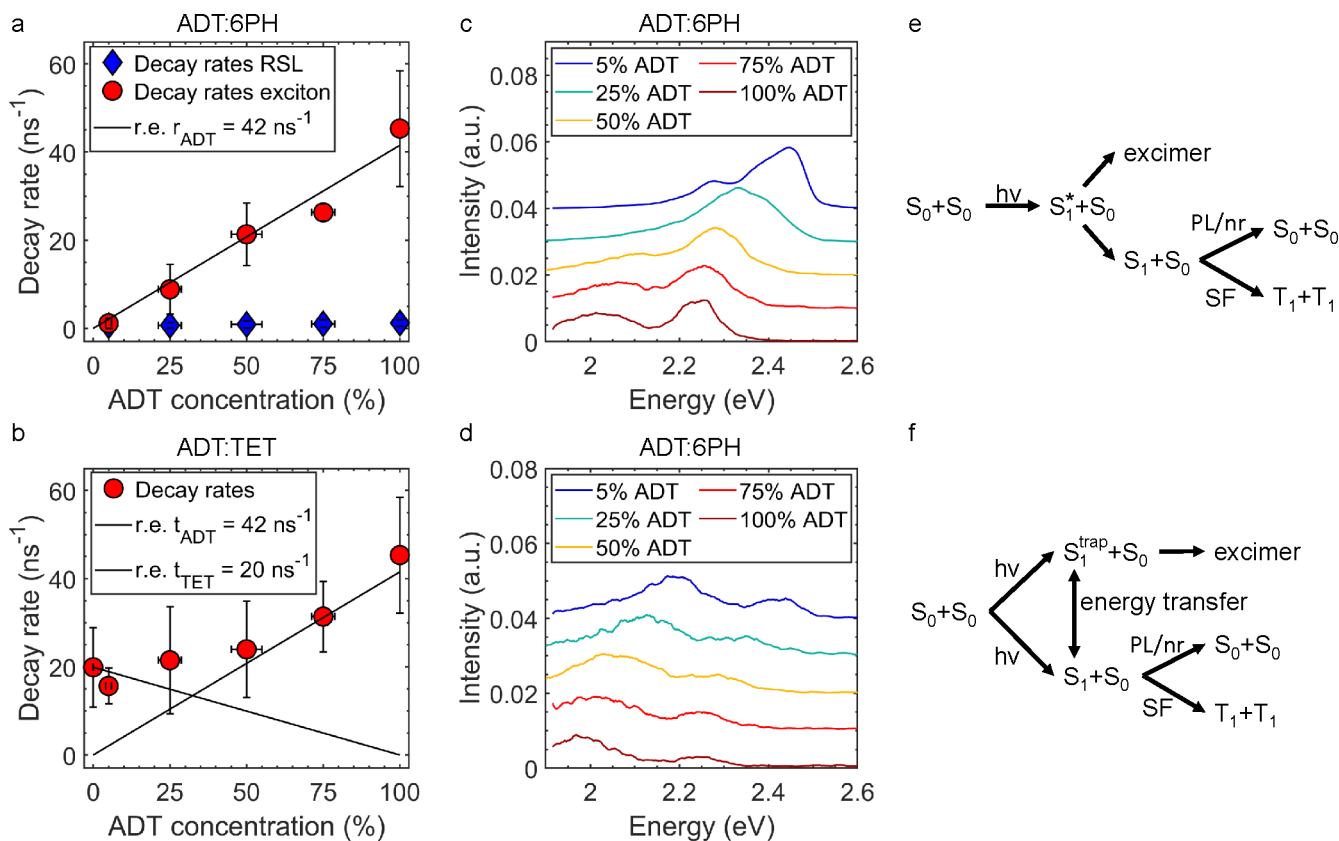


Figure 4. (a,b) Evolution of the SF rate and RSL decay rate of ADT:6PH (a) and ADT:TET (b) blends. For SF based on incoherent population transfer a linear behavior with changing ADT concentration is expected according to the replacement effect (r.e.) as sketched in the graphs. Note that the decay rate for 5% ADT in (a) might be dominated by the decay of excitons on isolated ADT molecules and that the decay rate for 100% ADT in (a,b) is close to the instrument resolution, which is 10 ps. (c,d) Time-integrated PL spectra of ADT:6PH blends in the time range (c) 0 to 2 ns and (d) >4 ns (100%, 75% ADT), >8 ns (50% ADT), >40 ns (25%, 5% ADT). Excitation at 400 nm, data noise filtered and vertically offset for clarity. (e,f) Sketches of possible decay mechanisms.

shift of the RSL to lower energies with increasing time (compare Figure 4c and Figure 4d). This points toward the existence of energetically low-lying sites such as grain boundaries where X_{RSL} is long-lived^{51,54} and which are populated via exciton diffusion, dominating the spectrum at late times. Importantly, the simultaneous observation of exciton emission and RSL at short times indicates that X_{RSL} can also be formed within crystalline domains of the polycrystalline mixed films, i.e., is not unique to defect sites. However, the low-lying defect sites provide an additional decay channel via exciton diffusion, leading to the observed red shift of the RSL. This interpretation is supported by Figure 2c, where the change in peak positions of the RSL in the late time window with changing ADT concentration is also shown. We find the same trend as in the steady state PL data, suggesting that X_{RSL} exhibits the same sensitivity on changes in the polarizability of the local molecular environment, independent of the time window, and, thus, also a high CT admixture, indicating that it is the same state in both time windows.

Based on these results and in particular considering the different response of the two decay channels (exciton vs RSL) to changes in the polarizability, we can now discuss the nature of X_{RSL} and its role in the SF of ADT. The most important result is its dependence on the polarizability of the local molecular environment, for which we use the change in the energy of the free exciton emission as a measure. When Figure 2c and d are compared, clearly, both the free exciton emission

and the RSL follow similar trends with decreasing ADT concentration and changes in the band gap of the codeposited compound. As discussed before, the main reason for the shift in energy of the exciton emission is a change in the polarizability of the local molecular environment, and the same reasoning has also been applied to the shift in RSL energy. However, plotting both shifts against each other gives interesting insight into the above-mentioned CT state admixture to X_{RSL} .^{49,50} It allows us now to elucidate the nature of X_{RSL} and, in particular, to distinguish between an excimer and the triplet-pair state (¹(TT)) as possible origins. The former is expected to be highly sensitive to changes in polarizability due to a large CT admixture.² Consequently, the corresponding shift in the energetic position of the excimer emission with changing mixing ratio (and, thus, changing polarizability of the local molecular environment) should be larger than that of the free exciton emission and the slope in Figure 2e becomes >1 . For the second case, in order to understand the sensitivity of the ¹(TT) state to changes in the polarizability, the exact nature of this state has to be discussed first. The ¹(TT) state consists of not only two triplets but also a small admixture of other states, for example of the CT state,^{55,56} making the sensitivity of the ¹(TT) state to changes in the polarizability slightly higher than that of uncorrelated triplets.⁵⁰ However, the admixture of these states can be considered small for several reasons. From a theoretical standpoint, calculations on pentacene^{37,55} and tetracene⁵⁶

only showed a small admixture of these states to the ${}^1(\text{TT})$ state and since SF is occurring via the coherent mechanism in pentacene,⁵² while, in contrast, we showed that in ADT the incoherent SF mechanism is driving SF, it can be expected that the admixture of these states is even smaller in ADT than in pentacene.⁵⁷ Additionally, from an experimental viewpoint, a large admixture of such states to ${}^1(\text{TT})$ would make the ${}^1(\text{TT})$ state visible in absorption and photoluminescence spectroscopy without the need for Herzberg–Teller coupling,⁵⁵ which, however, contrasts with our results. Also, a large admixture would result in a high binding energy between the two triplets in the ${}^1(\text{TT})$ state, which would result in clear differences of the excited state absorption fingerprints between ${}^1(\text{TT})$ and uncorrelated triplets. However, previous studies on comparable singlet fission chromophores revealed that it is generally very challenging to find spectroscopic differences between these two.¹² For such states like ${}^1(\text{TT})$, which have a dominant triplet pair contribution and only a small CT state admixture, the energetic position of the corresponding emission is expected to be more stable upon changes in the polarizability of the local molecular environment due to a stronger localization of the corresponding excitation. Hence, if X_{RSL} was of ${}^1(\text{TT})$ nature, a slope ≤ 1 would be expected in Figure 2e. Clearly, the slope in Figure 2e is larger than 1, unambiguously demonstrating that X_{RSL} , the state related to this RSL, has a large CT state admixture and, thus, is of excimeric rather than of ${}^1(\text{TT})$ character.

Now, after X_{RSL} was identified as an excimer, the remaining question is whether it mediates SF or is a loss channel. We can rule out the excimer as the mediating species based on the lack of a concomitant increase of excimer luminescence on the time scale of the exciton decay (see Figure 3c,d). Instead, two scenarios for the interrelation of excimer formation and SF are proposed (see Figure 4e,f). In the first scenario photoexcitation leads to a nonrelaxed S_1 state, from where either ultrafast exciton relaxation to the free exciton band, followed by SF, or excimer formation can occur (Figure 4e). The second scenario assumes that excimer formation is facilitated at trap sites such as grain boundaries, while for the other sites SF is the dominant decay channel (Figure 4f). Since pronounced excimer emission is also observed in single crystals (see Supporting Information, Figure S7), despite the lack of grain boundaries and presumably a lower density of trap sites, the scenario in Figure 4e is favored. Importantly, neither the formation nor the decay of this excimer directly affects the SF process, suggesting neither a direct competition between SF and excimer formation nor a mediation of SF by the excimer state in ADT, but instead the coexistence of two parallel channels at room temperature.

CONCLUSIONS

In conclusion, ADT blends with weakly interacting spacer molecules are a promising approach to clarify the origin of RSL features in PL spectra of SF materials. They allow us to clearly distinguish contributions from excimer and triplet-pair state emission based on their different response to changes in the polarizability of the local molecular environment and, thus, shed light on a current debate about the role of emissive states in molecular systems that undergo SF. Generally, this approach can be used to clarify the nature of RSL states in a variety of chromophores.

ASSOCIATED CONTENT

SI Supporting Information

The Supporting Information is available free of charge at <https://pubs.acs.org/doi/10.1021/acs.jpcc.1c09297>.

Details on the structural analysis, X-ray diffraction data, absorption spectra and details on the TRPL spectra of ADT in solution and blends with 5% ADT and 25% ADT. (PDF)

AUTHOR INFORMATION

Corresponding Authors

Christopher J. Bardeen – Department of Chemistry, U.C. Riverside, Riverside, California 92521, United States;  orcid.org/0000-0002-5755-9476; Email: christob@ucr.edu

Katharina Broch – Institut für Angewandte Physik, Universität Tübingen, 72076 Tübingen, Germany;  orcid.org/0000-0002-9354-292X; Email: brochkatharina@gmail.com

Authors

Julian Hausch – Institut für Angewandte Physik, Universität Tübingen, 72076 Tübingen, Germany

Adam J. Berges – Department of Chemistry, U.C. Riverside, Riverside, California 92521, United States;  orcid.org/0000-0001-8586-9044

Clemens Zeiser – Institut für Angewandte Physik, Universität Tübingen, 72076 Tübingen, Germany;  orcid.org/0000-0003-3613-2243

Tim Rammel – Institut für Physikalische und Theoretische Chemie, 72076 Tübingen, Germany

Arne Morlok – Institut für Angewandte Physik, Universität Tübingen, 72076 Tübingen, Germany

Jona Bredehöft – Institut für Angewandte Physik, Universität Tübingen, 72076 Tübingen, Germany

Sebastian Hammer – Lehrstuhl für Experimentelle Physik VI, Julius-Maximilians Universität Würzburg, 97074 Würzburg, Germany;  orcid.org/0000-0002-0458-4133

Jens Pflaum – Lehrstuhl für Experimentelle Physik VI, Julius-Maximilians Universität Würzburg, 97074 Würzburg, Germany;  orcid.org/0000-0001-5326-8244

Complete contact information is available at:

<https://pubs.acs.org/10.1021/acs.jpcc.1c09297>

Notes

The authors declare no competing financial interest.

ACKNOWLEDGMENTS

J.H. and K.B. thank Prof. Schreiber (University of Tuebingen) for access to equipment. J.H. and K.B. acknowledge funding by the German Research Foundation (BR4869/4-1). C.J.B. acknowledges support by the U.S. National Science Foundation, Grant CHE-1800187. J.P. and S.H. acknowledge support by the Bavarian State Ministry for Science and the Arts within the collaborative research network “Solar Technologies go Hybrid” (SolTech).

REFERENCES

- (1) He, R.; Chi, X.; Pinczuk, A.; Lang, D.; Ramirez, A. P. Extrinsic optical recombination in pentacene single crystals: Evidence of gap states. *Appl. Phys. Lett.* **2005**, *87*, 211117.
- (2) Birks, J. B. Excimers. *Rep. Prog. Phys.* **1975**, *38*, 903.

(3) Hanna, M. C.; Nozik, A. J. Solar conversion efficiency of photovoltaic and photoelectrolysis cells with carrier multiplication absorbers. *J. Appl. Phys.* **2006**, *100*, No. 074510.

(4) Smith, M. B.; Michl, J. Recent Advances in Singlet Fission. *Annu. Rev. Phys. Chem.* **2013**, *64*, 361–386.

(5) Seiler, H.; Krynski, M.; Zahn, D.; Hammer, S.; Windsor, Y. W.; Vasileiadis, T.; Pflaum, J.; Ernstorfer, R.; Rossi, M.; Schwoerer, H. Nuclear dynamics of singlet exciton fission in pentacene single crystals. *Sci. Adv.* **2021**, *7*, No. eabg0869.

(6) Birech, Z.; Schwoerer, M.; Schmeiler, T.; Pflaum, J.; Schwoerer, H. Ultrafast dynamics of excitons in tetracene single crystals. *J. Chem. Phys.* **2014**, *140*, 114501.

(7) Wilson, M. W. B.; Rao, A.; Clark, J.; Kumar, R. S. S.; Brida, D.; Cerullo, G.; Friend, R. H. Ultrafast Dynamics of Exciton Fission in Polycrystalline Pentacene. *J. Am. Chem. Soc.* **2011**, *133*, 11830–11833.

(8) Sanders, S. N.; Pun, A. B.; Parenti, K. R.; Kumarasamy, E.; Yablon, L. M.; Sfeir, M. Y.; Campos, L. M. Understanding the Bound Triplet-Pair State in Singlet Fission. *Chem.* **2019**, *5*, 1988–2005.

(9) Burdett, J. J.; Bardeen, C. J. Quantum Beats in Crystalline Tetracene Delayed Fluorescence Due to Triplet Pair Coherences Produced by Direct Singlet Fission. *J. Am. Chem. Soc.* **2012**, *134*, 8597–8607.

(10) Burdett, J. J.; Gosztola, D.; Bardeen, C. J. The dependence of singlet exciton relaxation on excitation density and temperature in polycrystalline tetracene thin films: Kinetic evidence for a dark intermediate state and implications for singlet fission. *J. Chem. Phys.* **2011**, *135*, 214508.

(11) Piland, G. B.; Bardeen, C. J. How morphology affects singlet fission in crystalline tetracene. *J. Phys. Chem. Lett.* **2015**, *6*, 1841–1846.

(12) Stern, H. L.; Musser, A. J.; Gelinis, S.; Parkinson, P.; Herz, L. M.; Bruzek, M. J.; Anthony, J.; Friend, R. H.; Walker, B. J. Identification of a triplet pair intermediate in singlet exciton fission in solution. *P. Natl. Acad. Sci.* **2015**, *112*, 7656–7661.

(13) Bossanyi, D. G.; Matthiesen, M.; Wang, S.; Smith, J. A.; Kilbride, R. C.; Shipp, J. D.; Chekulaev, D.; Holland, E.; Anthony, J. E.; Zaumseil, J.; et al. Emissive spin-0 triplet-pairs are a direct product of triplet–triplet annihilation in pentacene single crystals and anthradithiophene films. *Nat. Chem.* **2021**, *13*, 163–171.

(14) Dover, C.; Gallaher, J.; Frazer, L.; Tapping, P.; Petty, A.; Crossley, M.; Anthony, J.; Kee, T.; Schmidt, T. Endothermic singlet fission is hindered by excimer formation. *Nat. Chem.* **2018**, *10*, 305–310.

(15) Cruz, C. D.; Chronister, E. L.; Bardeen, C. J. Using temperature dependent fluorescence to evaluate singlet fission pathways in tetracene single crystals. *J. Chem. Phys.* **2020**, *153*, 234504.

(16) Tayebjee, M. J. Y.; Clady, R. G. C. R.; Schmidt, T. W. The exciton dynamics in tetracene thin films. *Phys. Chem. Chem. Phys.* **2013**, *15*, 14797–14805.

(17) Zimmerman, P.; Bell, F.; Casanova, D.; Head-Gordon, M. Mechanism for Singlet Fission in Pentacene and Tetracene: From Single Exciton to Two Triplets. *J. Am. Chem. Soc.* **2011**, *133*, 19944–19952.

(18) Musser, A. J.; Clark, J. Triplet-Pair States in Organic Semiconductors. *Annu. Rev. Phys. Chem.* **2019**, *70*, 323–351.

(19) Thampi, A.; Stern, H. L.; Cheminal, A.; Tayebjee, M. J. Y.; Petty, A. J.; Anthony, J. E.; Rao, A. Elucidation of excitation energy dependent correlated triplet pair formation pathways in an endothermic singlet fission system. *J. Am. Chem. Soc.* **2018**, *140*, 4613–4622.

(20) Yong, C. K.; Musser, A. J.; Bayliss, S. L.; Lukman, S.; Tamura, H.; Bubnova, O.; Hallani, R. K.; Meneau, A.; Resel, R.; Maruyama, M.; et al. The entangled triplet pair state in acene and heteroacene materials. *Nat. Commun.* **2017**, *8*, 1–12.

(21) Kolata, K.; Breuer, T.; Witte, G.; Chatterjee, S. Molecular packing determines singlet exciton fission in organic semiconductors. *ACS Nano* **2014**, *8*, 7377–7383.

(22) Feng, X.; Krylov, A. I. On couplings and excimers: lessons from studies of singlet fission in covalently linked tetracene dimers. *Phys. Chem. Chem. Phys.* **2016**, *18*, 7751–7761.

(23) Liu, H.; Nichols, V. M.; Shen, L.; Jahansouz, S.; Chen, Y.; Hanson, K. M.; Bardeen, C. J.; Li, X. Synthesis and photophysical properties of a “face-to-face” stacked tetracene dimer. *Phys. Chem. Chem. Phys.* **2015**, *17*, 6523–6531.

(24) Ni, W.; Sun, L.; Gurzadyan, G. G. Ultrafast spectroscopy reveals singlet fission, ionization and excimer formation in perylene film. *Sci. Rep.* **2021**, *11*, 5220.

(25) Dron, P. I.; Michl, J.; Johnson, J. C. Singlet fission and excimer formation in disordered solids of alkyl-substituted 1,3-diphenylisobenzofurans. *J. Phys. Chem. A* **2017**, *121*, 8596–8603.

(26) Ye, C.; Gray, V.; Mårtensson, J.; Börjesson, K. Annihilation versus excimer formation by the triplet pair in triplet–triplet annihilation photon upconversion. *J. Am. Chem. Soc.* **2019**, *141*, 9578–9584.

(27) Miller, C. E.; Wasielewski, M. R.; Schatz, G. C. Modeling singlet fission in rylene and diketopyrrolopyrrole derivatives: The role of the charge transfer state in superexchange and excimer formation. *J. Phys. Chem. C* **2017**, *121*, 10345–10350.

(28) Mauck, C. M.; Hartnett, P. E.; Margulies, E. A.; Ma, L.; Miller, C. E.; Schatz, G. C.; Marks, T. J.; Wasielewski, M. R. Singlet fission via an excimer-like intermediate in 3,6-bis(thiophen-2-yl)-diketopyrrolopyrrole derivatives. *J. Am. Chem. Soc.* **2016**, *138*, 11749–11761.

(29) Walker, B. J.; Musser, A. J.; Beljonne, D.; Friend, R. H. Singlet exciton fission in solution. *Nat. Chem.* **2013**, *5*, 1019–1024.

(30) Dean, J. C.; Zhang, R.; Hallani, R. K.; Pensack, R. D.; Sanders, S. N.; Oblinsky, D. G.; Parkin, S. R.; Campos, L. M.; Anthony, J. E.; Scholes, G. D. Photophysical characterization and time-resolved spectroscopy of a anthradithiophene dimer: exploring the role of conformation in singlet fission. *Phys. Chem. Chem. Phys.* **2017**, *19*, 23162–23175.

(31) Young, R. M.; Wasielewski, M. R. Mixed electronic states in molecular dimers: Connecting singlet fission, excimer formation, and symmetry-breaking charge transfer. *Acc. Chem. Res.* **2020**, *53*, 1957–1968.

(32) Schrauben, J. N.; Ryerson, J. L.; Michl, J.; Johnson, J. C. Mechanism of singlet fission in thin films of 1,3-diphenylisobenzofuran. *J. Am. Chem. Soc.* **2014**, *136*, 7363–7373.

(33) Sandoval-Salinas, M. E.; Casanova, D. The doubly excited state in singlet fission. *ChemPhotoChem.* **2021**, *5*, 282–293.

(34) Huang, Y.; Buyanova, I. A.; Phansa, C.; Sandoval-Salinas, M. E.; Casanova, D.; Myers, W. K.; Greenham, N. C.; Rao, A.; Chen, W. M.; Puttisong, Y. Competition between triplet pair formation and excimer-like recombination controls singlet fission yield. *Cell Rep. Phys. Sci.* **2021**, *2*, 100339.

(35) Müller, U.; Roos, L.; Frank, M.; Deutsch, M.; Hammer, S.; Krumrein, M.; Friedrich, A.; Marder, T. B.; Engels, B.; Krueger, A.; et al. Role of Intermolecular Interactions in the Excited-State Photophysics of Tetracene and 2,2'-Ditetracene. *J. Phys. Chem. C* **2020**, *124*, 19435–19446.

(36) Zimmerman, P. M.; Zhang, Z.; Musgrave, C. B. Singlet fission in pentacene through multi-exciton quantum states. *Nat. Chem.* **2010**, *2*, 648–652.

(37) Zeng, T.; Hoffmann, R.; Ananth, N. The Low-Lying Electronic States of Pentacene and Their Roles in Singlet Fissions. *J. Am. Chem. Soc.* **2014**, *136*, 5755–5764.

(38) Herve, P.; Vandamme, L. General relation between refractive index and energy gap in semiconductors. *Infrared Phys. Techn.* **1994**, *35*, 609–615.

(39) Mamada, M.; Katagiri, H.; Mizukami, M.; Honda, K.; Minamiki, T.; Teraoka, R.; Uemura, T.; Tokito, S. Syn-/anti-anthradithiophene derivative isomer effects on semiconducting properties. *ACS Appl. Mater. Interfaces* **2013**, *5*, 9670–9677.

(40) Subramanian, S.; Park, S. K.; Parkin, S. R.; Podzorov, V.; Jackson, T. N.; Anthony, J. E. Chromophore Fluorination Enhances

Crystallization and Stability of Soluble Anthradithiophene Semiconductors. *J. Am. Chem. Soc.* **2008**, *130*, 2706–2707.

(41) Lloyd, M. T.; Mayer, A. C.; Subramanian, S.; Mourey, D. A.; Herman, D. J.; Bapat, A. V.; Anthony, J. E.; Malliaras, G. G. Efficient Solution-Processed Photovoltaic Cells Based on an Anthradithiophene/Fullerene Blend. *J. Am. Chem. Soc.* **2007**, *129*, 9144–9149.

(42) Jurchescu, O. D.; Subramanian, S.; Kline, R. J.; Hudson, S. D.; Anthony, J. E.; Jackson, T. N.; Gundlach, D. J. Organic Single-Crystal Field-Effect Transistors of a Soluble Anthradithiophene. *Chem. Mater.* **2008**, *20*, 6733–6737.

(43) Platt, A. D.; Day, J.; Subramanian, S.; Anthony, J. E.; Ostroverkhova, O. Optical, Fluorescent, and (Photo)conductive Properties of High-Performance Functionalized Pentacene and Anthradithiophene Derivatives. *J. Phys. Chem. C* **2009**, *113*, 14006–14014.

(44) Kwon, O.; Coropceanu, V.; Gruhn, N. E.; Durivage, J. C.; Laquindanum, J. G.; Katz, H. E.; Cornil, J.; Brédas, J. L. Characterization of the molecular parameters determining charge transport in anthradithiophene. *J. Chem. Phys.* **2004**, *120*, 8186–8194.

(45) Aufderheide, A.; Broch, K.; Novák, J.; Hinderhofer, A.; Nervo, R.; Gerlach, A.; Banerjee, R.; Schreiber, F. Mixing-induced anisotropic correlations in molecular crystalline systems. *Phys. Rev. Lett.* **2012**, *109*, 156102.

(46) Tanaka, S.; Miyata, K.; Sugimoto, T.; Watanabe, K.; Uemura, T.; Takeya, J.; Matsumoto, Y. Enhancement of the exciton coherence size in organic semiconductor by alkyl chain substitution. *J. Phys. Chem. C* **2016**, *120*, 7941–7948.

(47) Broch, K.; Dieterle, J.; Branchi, F.; Hestand, N. J.; Olivier, Y.; Tamura, H.; Cruz, C.; Nichols, V. M.; Hinderhofer, A.; Beljonne, D.; et al. Robust singlet fission in pentacene thin films with tuned charge transfer interactions. *Nat. Commun.* **2018**, *9*, 954.

(48) Beljonne, D.; Yamagata, H.; Brédas, J. L.; Spano, F. C.; Olivier, Y. Charge-transfer excitations steer the Davydov splitting and mediate singlet exciton fission in pentacene. *Phys. Rev. Lett.* **2013**, *110*, 226402.

(49) Yamagata, H.; Norton, J.; Hontz, E.; Olivier, Y.; Beljonne, D.; Brédas, J. L.; Silbey, R. J.; Spano, F. C. The nature of singlet excitons in oligoacene molecular crystals. *J. Chem. Phys.* **2011**, *134*, 204703.

(50) Marcus, R. A. On the theory of shifts and broadening of electronic spectra of polar solutes in polar media. *J. Chem. Phys.* **1965**, *43*, 1261–1274.

(51) Gao, Y.; Liu, H.; Zhang, S.; Gu, Q.; Shen, Y.; Ge, Y.; Yang, B. Excimer formation and evolution of excited state properties in discrete dimeric stacking of an anthracene derivative: a computational investigation. *Phys. Chem. Chem. Phys.* **2018**, *20*, 12129–12137.

(52) Zeiser, C.; Cruz, C.; Reichman, D. R.; Seitz, M.; Hagenlocher, J.; Chronister, E. L.; Bardeen, C. J.; Tempelaar, R.; Broch, K. Vacancy control in acene blends links exothermic singlet fission to coherence. *Nat. Commun.* **2021**, *12*, 5149.

(53) Arnold, S.; Alfano, R. R.; Pope, M.; Yu, W.; Ho, P.; Selsby, R.; Tharrats, J.; Swenberg, C. E. Triplet exciton caging in two dimensions. *J. Chem. Phys.* **1976**, *64*, 5104–5114.

(54) Casanova, D. Theoretical investigations of the perylene electronic structure: Monomer, dimers, and excimers. *Int. J. Quantum Chem.* **2015**, *115*, 442–452.

(55) Tempelaar, R.; Reichman, D. R. Vibronic exciton theory of singlet fission. I. Linear absorption and the anatomy of the correlated triplet pair state. *J. Chem. Phys.* **2017**, *146*, 174703.

(56) Morrison, A. F.; Herbert, J. M. Evidence for Singlet Fission Driven by Vibronic Coherence in Crystalline Tetracene. *J. Phys. Chem. Lett.* **2017**, *8*, 1442–1448.

(57) Alvertis, A. M.; Lukman, S.; Hele, T. J. H.; Fuemmeler, E. G.; Feng, J.; Wu, J.; Greenham, N. C.; Chin, A. W.; Musser, A. J. Switching between Coherent and Incoherent Singlet Fission via Solvent-Induced Symmetry Breaking. *J. Am. Chem. Soc.* **2019**, *141*, 17558–17570.

Recommended by ACS

Modulating Singlet Fission by Scanning through Vibronic Resonances in Pentacene-Based Blends

Frederik Unger, Katharina Broch, et al.

NOVEMBER 01, 2022

JOURNAL OF THE AMERICAN CHEMICAL SOCIETY

READ 

Effects of the Separation Distance between Two Triplet States Produced from Intramolecular Singlet Fission on the Two-Electron-Transfer Process

Heyuan Liu, Xiyou Li, et al.

AUGUST 05, 2022

JOURNAL OF THE AMERICAN CHEMICAL SOCIETY

READ 

Temperature-Dependent Recombination of Triplet Biexcitons in Singlet Fission of Hexacene

Yuqin Qian, Yi Rao, et al.

MAY 10, 2022

THE JOURNAL OF PHYSICAL CHEMISTRY C

READ 

Influence of Vibronic Coupling on Ultrafast Singlet Fission in a Linear Terryleneediimide Dimer

Jonathan D. Schultz, Michael R. Wasielewski, et al.

JANUARY 19, 2021

JOURNAL OF THE AMERICAN CHEMICAL SOCIETY

READ 

Get More Suggestions >